THE UNIVERSITY OF READING
Department of Meteorology

Undergraduate Finalists Project 2011/2012

The Steady-State Response of a Simple Tropical General Circulation Model to Seasonal Thermal Forcings

James Russell

The Steady-State Response of a Simple Tropical General Circulation Model to Seasonal Thermal Forcings

James Russell

The University of Reading

Department of Meteorology

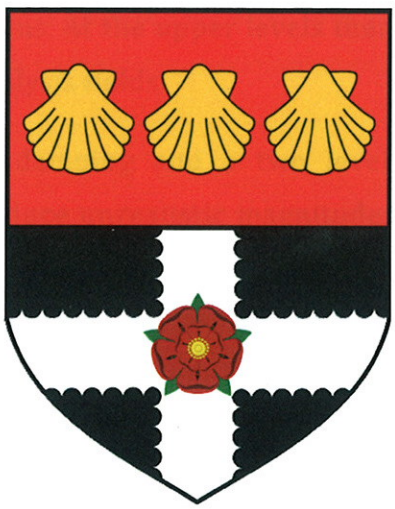

Submitted in partial fulfilment of the requirements of the degree of Masters in Meteorology, Meteorology with a year in Oklahoma, at the University of Reading, 14/03/2012.

Abstract

Shallow water equations are used in a grid point, two level model of the tropics to study the response to mean seasonal heating. The model implements several idealised forcing distributions that replicate heating in different seasons. An observed climatology of precipitation is used as a proxy for latent heating. This was incorporated into the model in order to study the response to a realistic, long term, climatological mean forcing with the aim of assessing tis capabilities.

Simulations with idealised forcing reproduce a number of characteristic regional tropical circulations such as the monsoons over India and Australia. These simulations showed encouraging results for further analysis of the model. Strong similarity is seen between simulations forced by observed seasonal heating and mean reanalysis circulation. Features such as the tropical upper level easterly jet, the flow associated with monsoons and the Pacific and Atlantic upper level westerly ducts are produced in the model. However, strong vector differences between model simulations and reanalysis data are observed in some regions. These occur in the lower levels around significant orographic features and where westerly jets are produced in model simulations. At the upper levels there is less agreement between model simulations and reanalysis fields.

A combination of average damping and a two level approximation during the derivation of the model produce unrealistic magnitudes of winds in both the upper and lower levels. The boundary condition used causes unrealistic circulation in the subtropics. A constant cooling was applied to the forcing field to test a proposed improvement of applying a global climatological average outgoing longwave cooling on the forcing. This improved the resolution of circulations in subtropical latitudes. With revisions, this model could provide a framework that allows simple modelling of tropical general circulation in response to heating.

1. Introduction

'There is no simple theoretical framework, analogous to quasi-geostrophic theory that can be used to provide an overall understanding of large-scale tropical motions.' (Holton, 2004)

Over the past few decades much research has been aimed at establishing a framework that reproduces large and regional scale tropical circulations. Many studies have simplified the tropical atmosphere to a steady state response of the forced, linearised shallow water equations (e.g. Webster 1972; Gill 1980). In these studies analytical solutions are obtained by forcing the equations with simple functions that parameterized heating and orography. Since then, this simple model established has formed a basis behind many analytical studies into tropical general circulation and atmospheric teleconnections (e.g. Roundy and Lynn, 2010; Lee et al., 2008). More recently, similar studies have attempted to observe the response of the general circulation to climate change-like thermal forcings (e.g. Butler, Thompson and Heikes, 2010). However, despite a surge in numerical modelling capability and remote sensing measurements of the tropics, the full capability and limitations of this simple model do not appear to have been explored in depth. Numerical methods provide a basis on which a complex observed climatology of atmospheric heating can be incorporated for use in a numerical version of the analytical model developed during the 1970's. While some studies use a numerical variation on this model none appear to have assessed its capabilities. Thus, considering its uses, it is important that the model be tested against modern spatially and temporally detailed data.

a) A Climatology of Tropical Heating

Basic principles behind the general circulation in the tropics date back to Halley (1686) and Hadley (1735). Halley theorised that the excess of heat in the tropics caused the air to become less 'ponderous' and rise. He stated that the rising air would be accompanied by a reversal of the flow aloft, while observing overall equator-ward flow at the surface, thus describing the meridionally orientated cell we now call the Hadley Circulation. Hadley (1735) elaborated on Halley's work by describing how conservation of angular momentum in the tropics produced the easterly trade winds. Many large scale motions

in tropical latitudes are not governed by conservation of angular momentum or linked to the circulation associated with the Hadley Cell. However, Halley's theory of diabatic heating, producing rising motion, with resultant horizontal flows still stands. In the tropics, large bodies of water and high temperatures, relative to that of higher latitudes, result in high evaporation rates and large exchanges of latent heat between the ocean and atmosphere. With the atmospheric boundary layer closer to saturation, the lifting condensation level is lowered, allowing convection to propagate more freely. As a result, convection is virtually ubiquitous throughout the tropics, resulting in large releases of latent heat, through condensation of water vapour to precipitation.

Webster (1972) uses estimations from Katayama (1964) to show that at low latitudes latent heating is of an order of magnitude greater than that of the sensible heat in a heat budget for the low latitudes. Therefore, it is possible, to assume in an idealised situation, that sensible heating can be neglected at low latitudes. Diabatic heating however is not the only forcing of convection. Forcings include frontal lifting mechanisms and orography. Within the tropics baroclinic instabilities and thus frontal lifting mechanisms are absent due to the barotropic nature of the atmosphere at low latitudes. A number of significant orographic features such as the Andes, the East African highlands and the Himalayas intersect mean zonal and meridional flow. While these act as a forcing for some regional areas of convection they are not ubiquitous throughout the tropics. Therefore, in an idealised model of the tropics it is possible to assume that the dominant forcing of convection is diabatic heating.

Convective, latent heating (LE) in Wm^{-2} can be related to the rain rate through the equation:

$$LE \approx \frac{\rho_w L_c RR}{(1000)(86400)} \quad (1)$$

where L_c is the latent heat of condensation, 2.4×10^6 $Jkg^{-1}K^{-1}$, ρ_w is the density of liquid water, 1000 kgm^{-3} and RR is the rain rate in $mmday^{-1}$. 1000 and 86400 are conversion factors for rain rate and time to SI units. Precipitation rates can therefore be taken as a proxy for transfer of heat to the atmosphere. Figure 1 shows the 28 year (1979-2007) mean distribution of latent heating during the Northern Hemisphere winter (December, January and February, hereafter DJF) and summer (June, July and August, hereafter JJA).

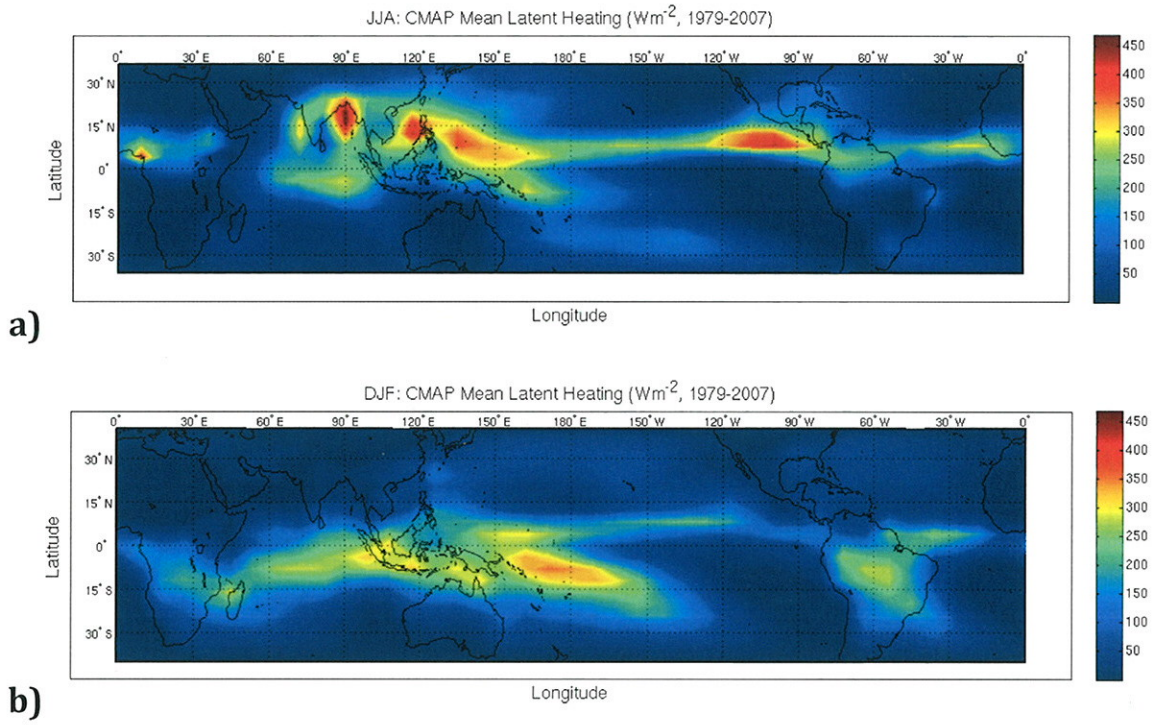

Figure 1: Mean distributions of precipitation converted to latent heating using equation 1. Latent heats given in tropical atmosphere (40S to 40N) and data is taken from the CMAP data set. Figures indicate a) JJA and b) DJF seasons respectively.

b) Tropical Circulation

Convection described as 'virtually ubiquitous' throughout the tropics is a result of the inter-tropical convergence zone (ITCZ) first described by Halley (1668). At the ITCZ, easterly trades are observed to turn creating a mean convergent meridional surface flow associated with the rising branch of the Hadley Cell. This line of convection is by no means spatially or temporally constant. As explained by Holton (2004) convection excites equatorial waves which communicate the effects over large longitudinal distances. These in turn produce regional synoptic scale responses. Through low level moisture convergence (divergence) associated with these responses, there is a strengthening (weakening) of areas of convection within the ITCZ.

As observed in Houze et al. (2000), equatorial waves as a response to deep areas of convection are commonly seen in the form of a couplet of equatorially trapped Kelvin and Rossby waves. An easterly progressing Kelvin wave is observed to induce easterly winds travelling toward the area of convection. Flow rounds the counter rotating gyres of the Rossby waves that form to the west of the region of convection, either side of the

equator. A strong convergent meridional flow forms and converges into a westerly jet near the centre of the region of convection.

The motion of the ITCZ over land areas results in specific flows associated with the monsoons. Monsoonal flow is a result of the enhanced area of precipitation occurring over land masses to the pole-ward side of warm equatorial oceans. A reversal in the land-ocean temperature gradient during the summer season leads to a synoptic scale 'sea breeze' whereby surface flow turns onshore driving a component of the ITCZ over a land mass. The characteristic flow of a monsoon is that of a strong reversal in the wind. While the Indian Monsoon is most prominent, monsoons also arise over South East Asia and Western Africa during the JJA season and in Northern Australia during the DJF season.

Although there are many regional circulations in the tropics these are the most prominent thermally driven synoptic circulations of the tropics and thus those discussed in further sections.

c) Simple Models of the Tropics

Another simple circulation formed by deep convective regions is the conceptual model of flow in the vertical and zonal directions of the Walker Cell, described by Bjerknes (1969). Easterly trade winds drive warm sea surface temperatures (SST's) west forming a warm pool in the western Pacific near Australia, Indonesia and South East Asia. This warm pool intensifies convection in the region. Consequential rising air reaches the tropopause, where it turns back towards the east as westerlies. Over the eastern Pacific, cold SST's cool the air at the surface causing divergent motion, where the upper level westerlies descend to complete the Walker Cell. As Halley (1686) theorised, in the vertical, horizontal tropical flow has an approximate structure whereby the flow in the upper troposphere is approximately the reversal of that of the lower troposphere. Conceptual circulations described, such as the Hadley Cell (Holton, 2004) and the Walker Cell (Bjerknes, 1969) support the possibility of a two layer assumption for a simple model.

Webster (1972) produced an analytical linear model based on the primitive equations given by Phillips (1963). This model used only two levels in the vertical. Motions were damped using simple dissipative mathematical terms and the model is initialised with

some basic currents. Simple forcing is applied by basic parameterizations of orography and latent heating in order to test the hypothesis that much of the time independent flows are a result of these. Through comparisons to other studies and observed fields, Webster (1972) concluded that much of the circulation in the tropics is forced by heating and orography.

Gill (1980) produced a similar analytical model in order to illustrate the response of the tropical atmosphere to some simple distributions of diabatic heating. The analytical model developed uses the forced shallow water equations on an equatorial beta plane. Some simple dissipative processes are included in order to study the atmosphere in a steady state flow. The model is initialised from a resting basic state. The response of the model to a number of distributions of heating is examined. The first is a symmetric (about the equator) region of diabatic heating that produces the equatorial Kelvin-Rossby wave couplet shown in Figure 2. A Kelvin wave is shown to propagate east from the heating region. Separate Rossby waves in each hemisphere propagate west at a third the phase speed of the Kelvin wave. Gill equates this region to an idealised reproduction of the predominant convective latent heating over Indonesia during much of the annual cycle. Figure 2 shows how this pressure system induces winds equated to the easterly trades over the Pacific, with a westerly jet into a zone of heating over Indonesia. This is similar to that discussed with observations in Houze et al. (2000).

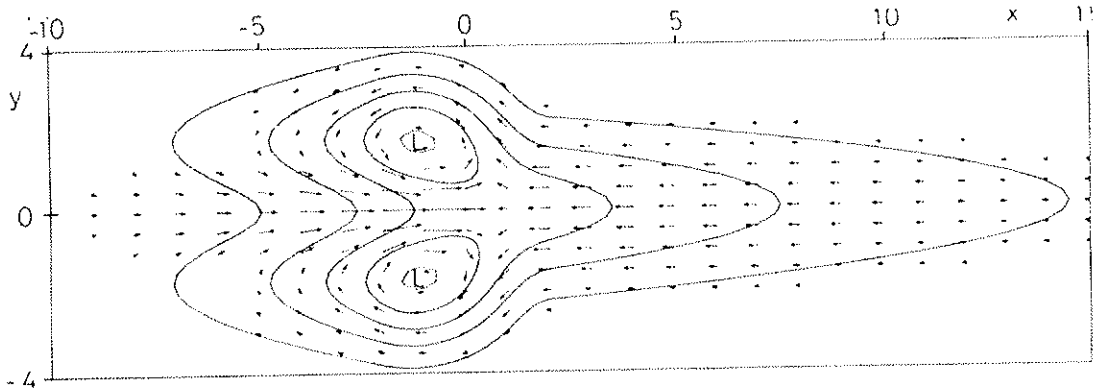

Figure 2: Circulation and pressure perturbation produced by a simple symmetric heating distribution in Gill (1980). x and y coordinates are in 1000's of km's from the centre of the heating region and from the equator respectively.

Another of Gill's analytical solutions is the circulation produced by a region of heating defined as a combination of the symmetric heat source and a zonally orientated line

source displaced north. Figure 3 depicts the solution of horizontal winds and vertical motion, produced by forcing the model with this combination.

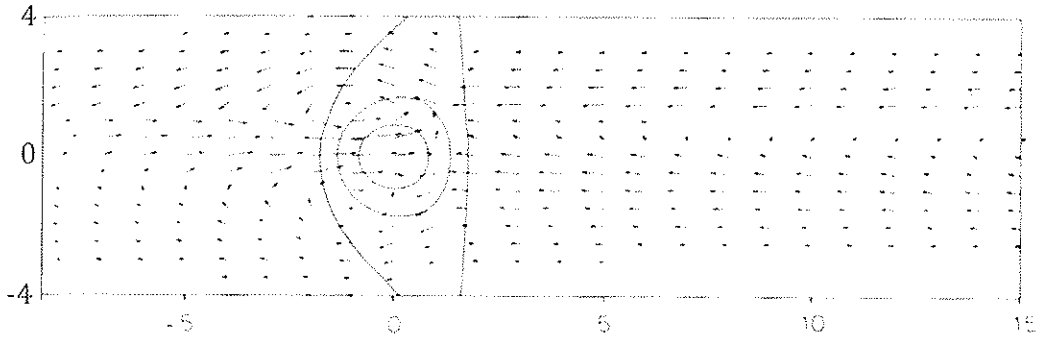

Figure 3: Circulation (arrows) produced by a combination of symmetric and line sources of heating (Gill, 1980). x and y coordinates are in 1000's of km's from the centre of the heating region and from the equator respectively. Vertical motion from the symmetric source is shown by contours.

Gill observes that the line source splits the easterlies into two separate jet structures with relatively weak flow between the line source and the equator. It is concluded that the shallow water equations, despite their simplicity, provide an 'illuminating' view of the tropical circulation.

It is aimed that this study will build on Gill's (1980) analytical solutions by answering the questions:

- How well does a numerical solution recreate Gill's analytical solutions?
- 'What regional circulation features does the model reproduce with an observed climatological latent heating distribution?
- What are the limitations of the model?

To answer these questions a numerical model, based on that in Gill (1980) is constructed using a set of discretised, linearized shallow water equations on a grid point model. Initially, the simple solutions produced in Gill are replicated with the aim of testing the numerical scheme against Gill's analytical solutions. These distributions are combined and developed into idealised seasonal pictures of heating allowing an examination of the response of the atmosphere to more complex, realistic distributions. A mean climatology of latent heating is produced from precipitation data converted using equation 1. This is built in to the model to represent observed distributions of heating. The wind and geopotential height fields at 850mb and 150mb are examined and compared to reanalysis mean winds for the same period.

2. Model Description and Methodology

a) Model

The model has spatial and temporal resolution and extent as in Table 1.

Table 1: Resolution and extent of the temporal and spacial scales of the model.

	Resolution	Extent
Zonal	9° Longitude (999 km)	Circumglobal
Meridional	4° Latitude (444 km)	40°N to 40°S
Vertical	850hPa and 150hPa	N/A
Temporal	1 hour (3600s)	Unlimited (images shown at 240 hours from initialisation).

A two layer assumption is used as discussed in Section 1 and perturbations in wind and geopotential height at 850hPa and 150hPa are found as shown in Figure 4.

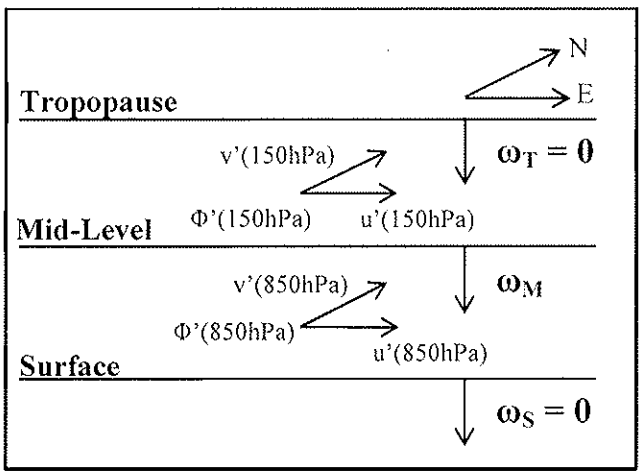

Figure 4: Three dimensional depiction of two layer model with indicated levels and directions of positive flow.

The equations used are the linearised shallow water equations on an equatorial beta plane. It is appropriate to use a beta plane approximation to simplify the equations as the coriolis parameter can be approximated with a constant gradient to approximately 40° either side of the equator.

The zonal and meridional momentum equations as in Holton 2004 are:

$$\frac{\partial u'}{\partial t} - \beta y v' + \frac{\partial \Phi'}{\partial x} = 0 \qquad (2)$$

$$\frac{\partial v'}{\partial t} + \beta y u' + \frac{\partial \Phi'}{\partial y} = 0 \qquad (3)$$

where u', v' and Φ' are the zonal and meridional perturbation to the winds and geopotential height respectively, β is the beta parameter (β=2.3×10^{-11}) relating to the

equatorial beta plane, t is time and x and y are distance in the zonal and meridional directions respectively. As a result of the beta plane approximation, curvature terms can be assumed small for motions on large length-scales thus the grid is assumed to be a flat plane.

In a two level model vertical velocity at the upper and lower bounds of the model (ω_T and ω_S) are zero as depicted in Figure 4. Therefore there is only exchange of mass between the two levels. The continuity equation in pressure coordinates can be given by:

$$\frac{\partial u}{dx} + \frac{\partial v}{dy} + \frac{\partial \omega}{dp} = 0 \tag{4}$$

where ω is the vertical velocity with respect to pressure (p).

Using a finite difference approximation in the vertical as in Figure 4 continuity becomes:

$$\frac{\partial u'_1}{dx} + \frac{\partial v'_1}{dy} = -\frac{\omega_M - \omega_T}{\Delta p} = -\frac{\omega_M}{\Delta p} \tag{5}$$

$$\frac{\partial u'_2}{dx} + \frac{\partial v'_2}{dy} = -\frac{\omega_S - \omega_M}{\Delta p} = \frac{\omega_M}{\Delta p} \tag{6}$$

It can be seen from these equations that the upper level can be modelled as a reversal of the lower level as equations 5 and 6 are satisfied if:

$$u'_1 = -u'_2 \tag{7}$$

$$v'_1 = -v'_2 \tag{8}$$

An equation predicting the evolution of geopotential height is derived by combining the continuity equation with the hydrostatic and thermodynamic equations given respectively by:

$$\frac{D\theta}{Dt} = Q \tag{9}$$

$$\frac{\partial \Phi}{dp} = -h\theta \tag{10}$$

where θ is the potential temperature, Q is a source of heat, Φ is the geopotential height and h is given by:

$$h(p) = \frac{R}{p}\left[\frac{p}{p_0}\right]^{\frac{R_d}{c_p}} \tag{11}$$

In this equation R is the universal gas constant, R_d is the gas constant for dry air p_0 is a reference pressure (1000hPa) and c_p is specific heat at constant pressure.

An equation defining geopotential height therefore has the form:

$$\frac{\partial \Phi'}{\partial t} + c_e^2 \left(\frac{\partial u'}{dx} + \frac{\partial v'}{dy} \right) = -AQ \tag{12}$$

where Q is the forcing (heating in this model) and:

$$c_e^2 = \frac{\sigma^2}{2} \Delta p^2 \tag{13}$$

$$A = \frac{h \Delta p}{2} \tag{14}$$

Here σ is the static stability parameter. Using a forward in time, centred in space (FTCS) finite difference approximation for the first time step and a centred in time, centred in space (CTCS) finite difference approximation for the following time steps, equations are obtained that can be iterated on a latitude-longitude grid. The following are the equations in CTCS form:

$$\Phi'_{t+1} = \Phi'_{t-1} + 2\Delta t \left(-AQ - c_e^2 \left(\frac{u'_{x+1} - u'_{x-1}}{2\Delta x} + \frac{v'_{x+1} - v'_{x-1}}{2\Delta y} \right) \right) + E\Phi'_t \tag{15}$$

$$u'_{t+1} = u'_{t-1} + 2\Delta t \left(f v_t' - \frac{\Phi'_{x+1} - \Phi'_{x-1}}{2\Delta x} \right) + E u'_t \tag{16}$$

$$v'_{t+1} = v'_{t-1} + 2\Delta t \left(-f u_t' - \frac{\Phi'_{x+1} - \Phi'_{x-1}}{2\Delta y} \right) + E v'_t \tag{17}$$

The final term in the equations represents a simple dissipation term given by 'Rayleigh Friction' and 'Newtonian Cooling' as described in Wu et al. (2000). The dissipation rate is given by E=0.03. This allows iterations of the equations to reach a steady state so that it is possible to observe the ultimate wind fields. Equations are coded in FORTRAN for compilation. To produce a circumglobal model, the equations are iterated for an extra longitude at each end of the grid domain and copied to the corresponding longitude in the grid. The model is initialised with a resting basic state and equations are iterated until they reach a steady state. As briefly discussed in Section 1 and in detail in Marshall and Plumb (2007), mid-latitude general circulation has relatively different forcings to that of the tropics. A poleward boundary is therefore included at 40N and 40S whereby forcing at latitudes is reduced to zero. This limits the model to tropical latitudes where

heating plays a major role. Setting forcing to zero here prevents numerical instabilities from occurring.

b) Methodology

Initially the simulations are forced by a simple symmetric distribution of latent heating analogous to Gill (1980). This has the form:

$$Q = \cos ki^2 \, e^{-\frac{\beta j^2}{a}} \tag{18}$$

where i is the longitudinal distance in km from the Greenwich Meridian, j is the latitudinal distance from the equator, a and b are latitudinal decay constants and k is the longitudinal wavenumber. Circulation patterns produced are analysed and compared to that of Gill's to verify the numerical iteration produces the same as that of the analytical solutions. An attempt to connect the circulation and pressure perturbation pattern to realistic flow patterns is made. The only other simple source shown here is a combined heating function. A heating function idealising the Monsoon in South East Asian longitudes is produced by displacing a symmetric function. This is combined with a zonally orientated line source of heating representing the ITCZ at 10N. This heating function is of the form:

$$Q = \sin ki^2 \, e^{-\frac{\beta(j+20°Latitude)^2}{a}} + e^{-\frac{\beta(j+10°Latitude)^2}{b}} \tag{19}$$

Simple distributions such as the above are combined to produce idealised distributions of latent heat release for the DJF and JJA seasons. A background field of $30Wm^{-2}$ (approximately 1mm/day) is applied to simple and idealised latent heating distributions to represent minimal heating in other regions. Additionally the heating is scaled so that the mean heating over the entire domain is equal to that of the mean heating in the observed fields. Comparisons are made to the following fields forced by observed latent heating distributions.

Observed latent heating distributions are given by the enhanced monthly mean CPC (Climate Prediction Center) merged analysis of precipitation data (CMAP) as given by Xie and Arkin (1997). CMAP merges rainfall estimates from a variety of satellite and ground-based sources, combined with the National Center for Environmental Prediction (NCEP) reanalysis, in order to produce a gridded worldwide distribution of

precipitation. Mean, monthly mean values of the full length of CMAP precipitation rates (28 years, 1979-2007) are calculated for DJF and JJA seasons. Using Equation 1 mean precipitation rate is converted from a rain rate in mm/day to a latent heating in Wm^{-2}. A bilinear interpolation is used to transpose latent heating on to the model grid. Model simulations are produced using observed latent heating as the forcing function (Q) as in equation 15. Heating close to the boundaries represents that of precipitation from trailing mid-latitude frontal systems. As discussed in Section 1 forcing of the general circulation in midlatitudes is different to that in the tropics. Thus, these bands of precipitation are not important in a heat budget in the tropics. Also, when heating is produced close to the boundary we produce numerical instabilities in the model. Therefore heating is 'phased out' close to the boundary by multiplying the farthest north and south four latitudes of latent heating by successively smaller fractions (i.e. 0.75, 0.5, 0.25 and the boundary condition sets heating to zero).

NCEP-NCAR Reanalysis data (hereafter reanalysis or observed) is used for comparison of the model simulations to a respective global climatological mean. The data set, as given in Kalnay et al. (1996) represents the state of the atmosphere since 1948. It is a joint product from NCEP and the National Center for Atmospheric Research (NCAR). Means of reanalysis monthly mean winds and thickness at 850hPa and 150hPa for DJF and JJA seasons over the period 1979-2007 are calculated. Figures are shown in Appendix A as reference is made to these throughout the text. These are transposed to the model grid using a bilinear interpolation. Vector differences are calculated for comparison to reanalysis winds by the equation:

$$\Delta U = U(\text{Model}) - U(\text{Reannalysis}) \tag{20}$$

where U is the vector wind and Δ represents the difference. Differences are calculated by first normalising the winds to account for an unphysical difference between the model and reanalysis winds discussed in Section 5. Formulas used are:

$$u' = u'/\max(u') \tag{21}$$

$$v' = v'/\max(u') \tag{22}$$

By producing non-dimensional normalised parameters a direct comparison between circulations is possible by discounting magnitude. Comparisons are also made to a number of different sources and theories.

Mean and standard deviations of the steady-state zonal and meridional wind fields simulated by the model and the reanalysis are computed to compare the overall magnitude of the model winds to the reanalysis. Finally, a constant cooling is applied to the heating function to represent longwave cooling. Some form of statistical test was proposed however, this would involve testing a large number of data sources against the model steady state flow for which we only have one set of climatological data.

3. Simple Latent Heating Functions

In this section the model response to two simple heating distributions is studied.

a) Model Simulation Forced by Symmetric Heating Function

A simulation of the model forced by the symmetric heating function, given by equation 18, is shown in Figure 5. This is an idealisation of the climatological average convective region over Indonesia during the DJF and Equinoctial seasons such as that in Gill (1980). The lower level geopotential height field (Figure 5b) shows the Kelvin-Rossby wave couplet which is similar to Gill's (1980) analytical solution. An equatorially trapped Kelvin wave propagates eastward (upstream) from the heating region. The wave dissipates as it propagates at a rate proportional to the dissipation rate (E). Over the Pacific, winds flow down pressure gradient toward the heating region. This flow, induced by the Kelvin wave, is characteristic of the mean zonal flow of easterlies that dominate the low level Pacific (Hastenrath, 1996) This confirms Gill's (1980) conclusions on his analytical solutions. At the onset of simulations, inflow at the centre of the heating region causes convergence. This results in mass transport to the upper levels where divergence of the flow is seen. This is as an effect of the two layer assumption with a reversal of the flow at upper levels. As the Kelvin wave begins to dominate the production of flow due to its relatively larger phase speed than other waves, easterlies become a prominent feature over much of the model domain. This causes a shear between the Kelvin wave induced easterlies and a westerly inflow into the heating region. This shear produces separate Rossby waves symmetric about the

equator, downstream of the heating zone. Shear induced intensification of the Rossby waves strengthens the westerly inflow.

The model produces numerical artefacts in the geopotential height field between 150°E and 180°E. This is in contrast to Gill's solution. However, these numerical artefacts do not appear to have any effect on the overall numerical solution.

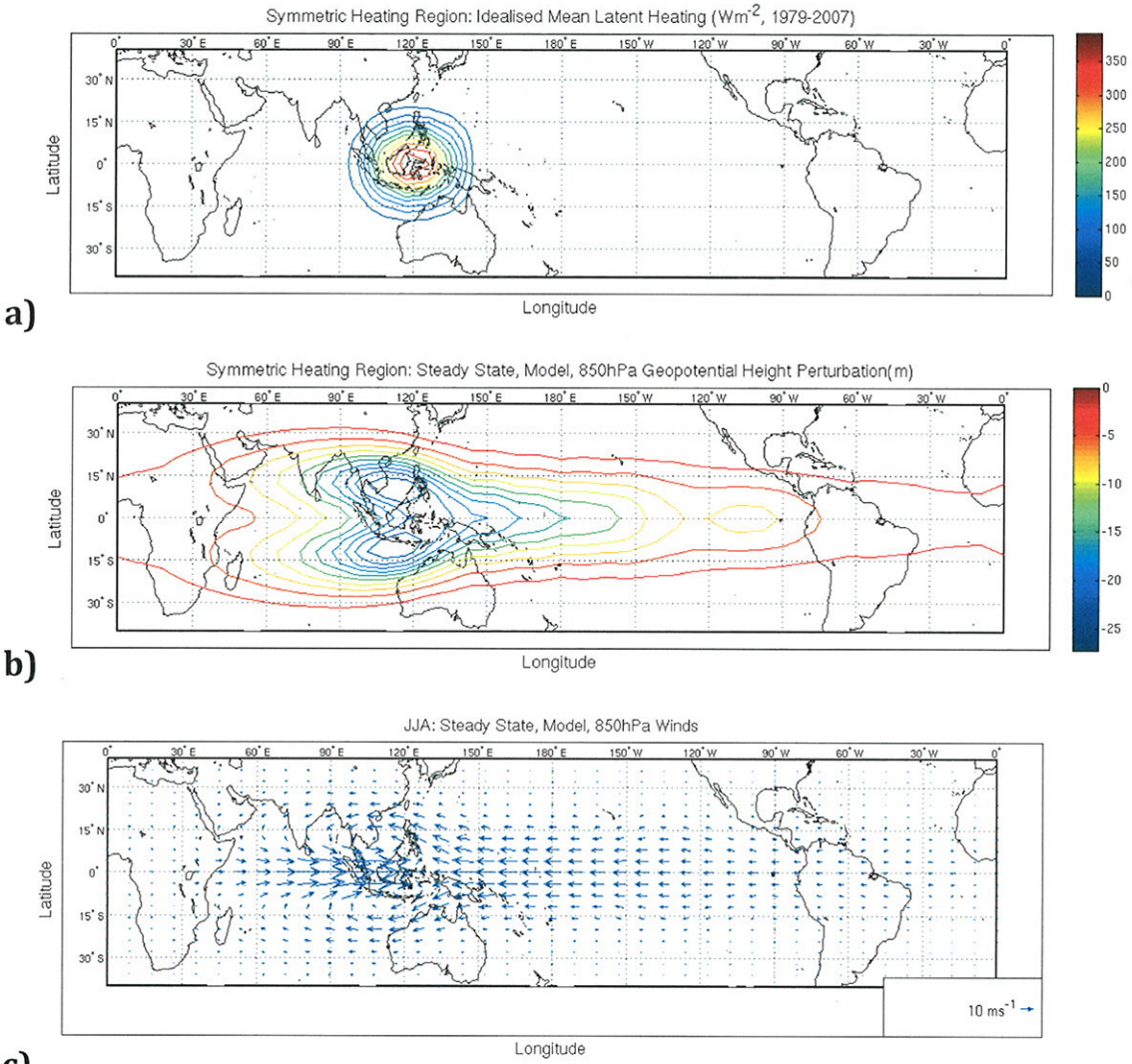

Figure 5: Model Simulation when forced by a symmetrical heating distribution similar to that in Gill (1980). Panels depict the simulation a) low level winds b) low level geopotential height and c) winds.

b) Model Simulation Forced by Combined Heating Distributions

Figure 6 shows a simulation produced by forcing the equations with a combined distribution as in Figure 6a. A line source of heating displaced to 10°N represents

convection in the ITCZ. A symmetric region of heating displaced to 20°N represents convection in the Indian Monsoon. A comparison of Figure 6a to Figure 1a shows that this distribution is an idealised distribution of heating for the JJA season.

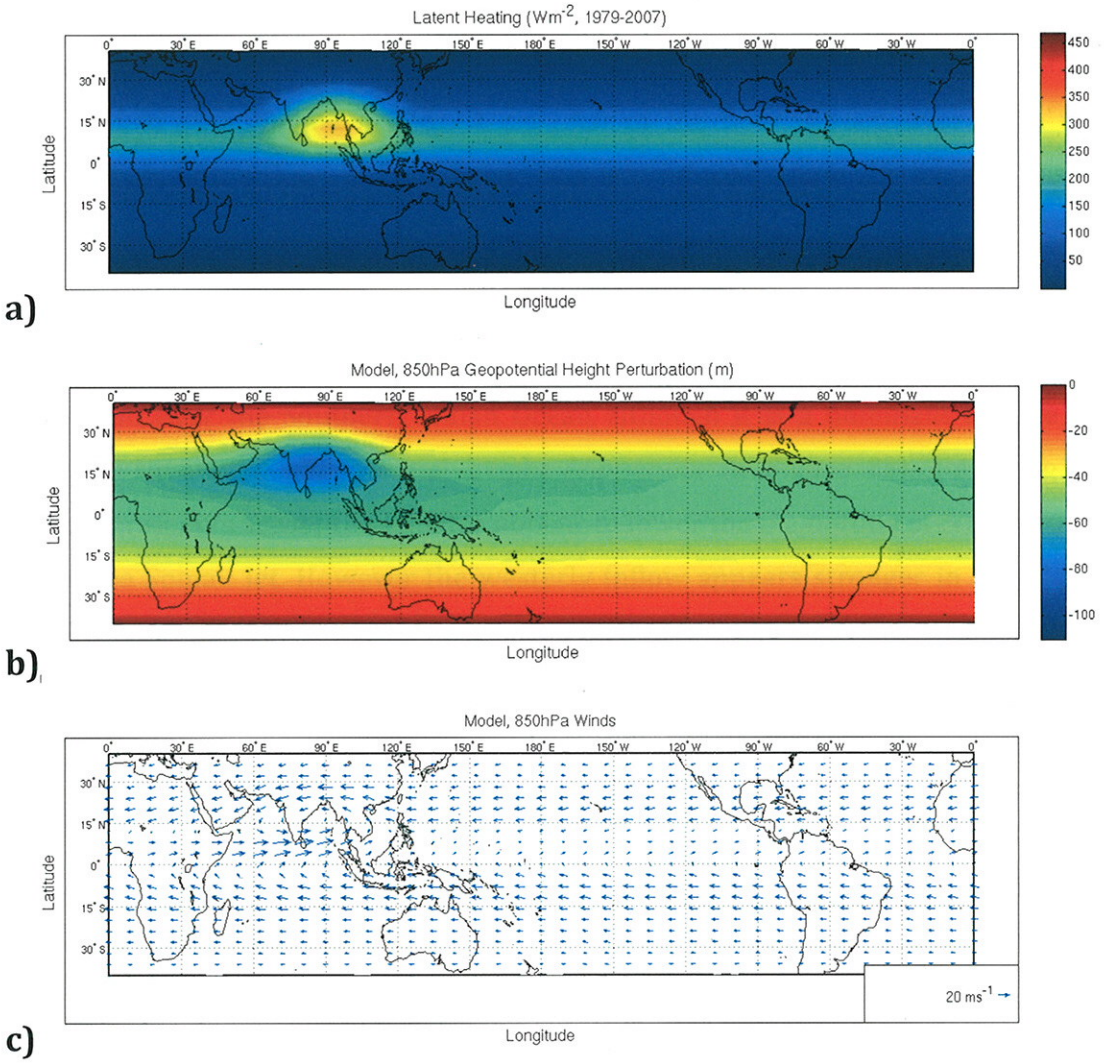

Figure 6: a) Combined heating distribution idealising the South-East Asian Monsoon and a line source of convergence representing the ITCZ with perturbations of lower level b) geopotential height and c) winds.

The geopotential height field in Figure 6b shows a relatively intense cyclonic pressure system similar to the climatological average low thickness produced by the South-East Asian Monsoon. This is embedded within a broad, zonally orientated equatorial trough. Flow patterns in Figure 6c show a cross equatorial flow produced by the idealised ITCZ with relatively light Westerlies between the equator and the source of heating. This is in

agreement with Gill's (1980) combined solution, documented in Section 1 that divides the easterly trade winds into two separate jets.

Over India, a strong westerly jet is observed into the centre of the zone of strengthened heating associated with the Monsoon. The Monsoon inflow produces an intensified cross equatorial flow. This is similar to the Somali jet during the JJA season documented by Krishnamurti and Bhalme (1976). A reversal of the flow is seen over India that is characteristic of the flow in a monsoon. This is produced where the tropical easterlies round the base of the Monsoonal trough over northern India.

No significant heat sources in the Southern Hemisphere result in a constant zonal average of meridional gradient in geopotential height. As a result the Mascarene High is not present over the Southern Indian Ocean although it is a dominant feature in the temporally averaged geopotential height (Appendix A: Figure 2a). Resulting lower pressure gradients across the Equator appear to lower the magnitude of cross equatorial flow in the Somali Jet. However the westerly inflow appears stronger in magnitude to that of the observed. This can be attributed to the decrease in surface friction due to a lack of parameterized orography in the East African plateau.

4. Idealised Seasonal Heating Functions

In this section the model response to idealised JJA (Figure 7) and DJF (Figure 8) heating functions are explored.

a) Model Simulation for JJA Season

A simulation forced by idealised JJA heating shows many of the same characteristics to that of the combined ITCZ and Monsoonal heating function. A dominant trough in the 850hPa geopotential height (Figure 7b) exists over India embedded within a broad equatorial trough that covers much of the equatorial Pacific. Contrary, to the combined heating function in Section 3, a weak trough exists over Central America. This induces a weak monsoonal circulation and westerly jet. It also produces weak cross equatorial flow with divergence off the equatorial coast of South America. Relative to observed winds, this monsoonal circulation is not seen. It is likely that in the observed flow, any circulation in this region is disrupted by the Andes.

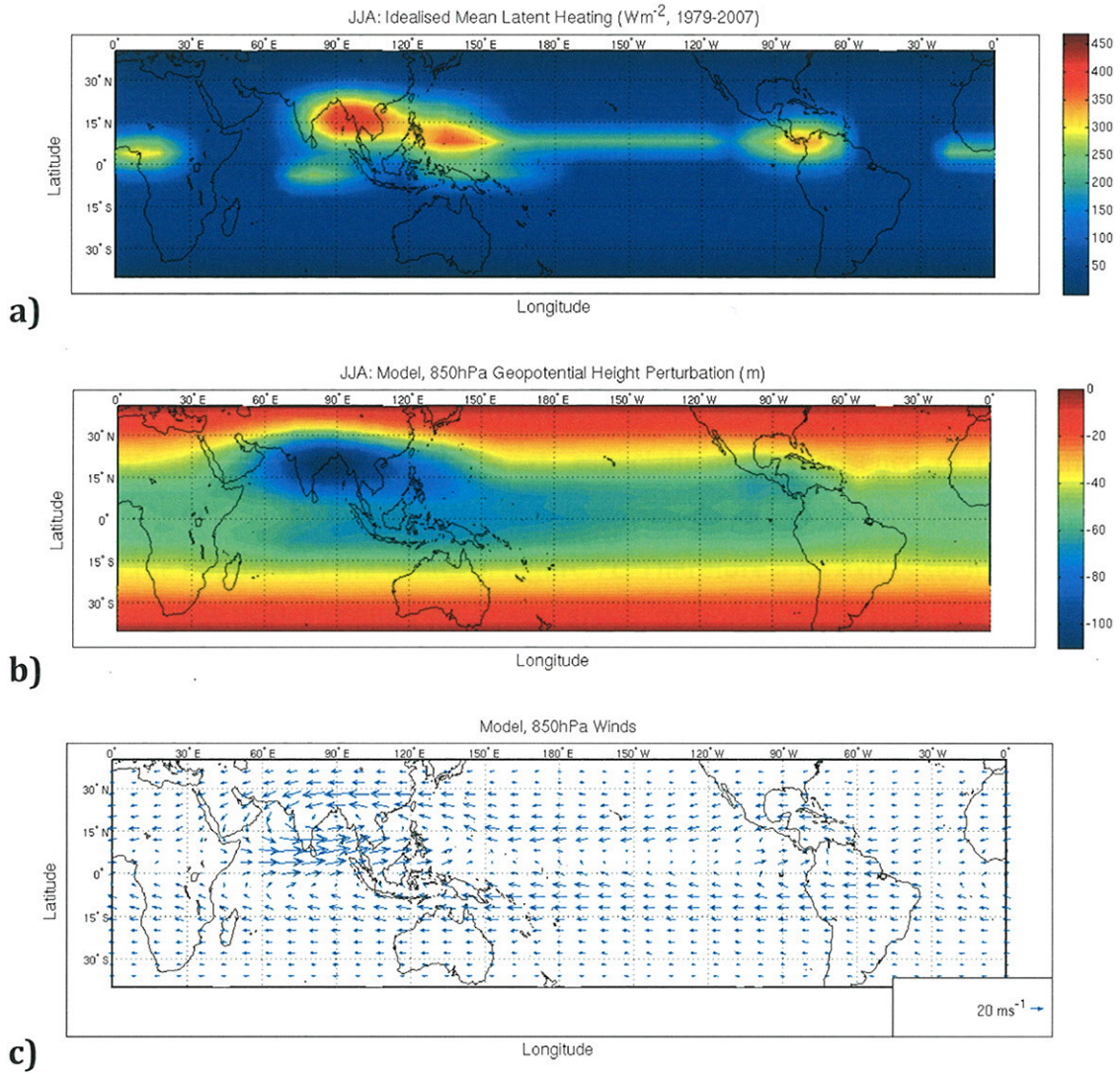

Figure 7: a) Idealised Heating distribution for JJA with the associated b) lower level geopotential height and c) wind.

The absence of forcing close to the boundaries produces an approximately constant zonally orientated belt of high pressure to exist over much of the subtropics in both hemispheres. This is also an effect of the boundary tending to zero. Exceptions to the constant subtropical high pressure belt produced occur where heating is further poleward. This is seen over South East Asia and to a lesser extent Central America in the Northern Hemisphere. A constant belt of high pressure is dissimilar to observed subtropical pressure systems such as those in Appendix A: Figure 2a.

Relative to simulations forced by the combined heating distribution in Section 1, a broader, deeper region of heating over South East Asia results in a broader Monsoonal trough. A stronger pressure gradient therefore produces stronger monsoonal inflow as

seen in Figure 7c. Displacement of the Monsoonal pressure system north also increases the magnitude of the Coriolis force acting on the winds in this region. Thus through gradient wind balance the winds increase. There also appears to be a strong meridional flow from the north intensifying the westerly inflow jet. This is not seen in the previous simulation or in the observed winds.

No monsoonal circulation is observed over Western Africa in association with the heating region in these longitudes. This is, in part, due to the relatively weak heating in the region as given by the heating function in Figure 7a. Also, this region is affected by strong monsoon convection to the west, especially in the absence of east African orography. As defined in Section 2, the flow is reversed aloft. Therefore 150hPa flow can be seen as the opposite of the winds in Figure 7c. Therefore a jet exit is seen with strong convergence aloft in the 150hPa flow over Africa. This appears to suppress the area of heating in Africa by causing weak divergence at the surface, a theory supported by Webster and Fasullo (2003).

b) Model Simulation for DJF Season

Figure 8 shows a simulation produced by forcing the model with an idealised DJF heating function. A broad equatorial trough covers most of the Pacific and Indian Oceans in low latitudes as shown in Figure 8b. A dominant trough over Indonesia and west Pacific longitudes in the Southern Hemisphere produces a strong low level westerly inflow jet over much of the Indian Ocean with weak cross equatorial flow to the North. This is associated with a broad band of heating in this region as shown in Figure 8a. Strong pressure gradients North and South of this trough induce strong Easterlies. A region of relatively low magnitude winds are observed in association with the idealised Indian Ocean ITCZ, separating the dominant easterlies from the westerly jet.

A second, weaker trough is centred on South American longitudes disconnected from the other by a ridge pushing north over the eastern Pacific. A jet-like structure of Easterlies is seen to produce wave features in these longitudes. Regions of heating in these longitudes produce weak areas of light convergent winds over South America with a region of weak divergence over the east Pacific close to the equator. Another subtropical ridge pushes north over the equatorial Atlantic. While the model simulation appears to resolve some of the subtropical ridges and troughs in the southern

hemisphere, much of the northern hemisphere is zonally symmetric. It is dominated by the easterly trade winds that are approximately constant with longitude.

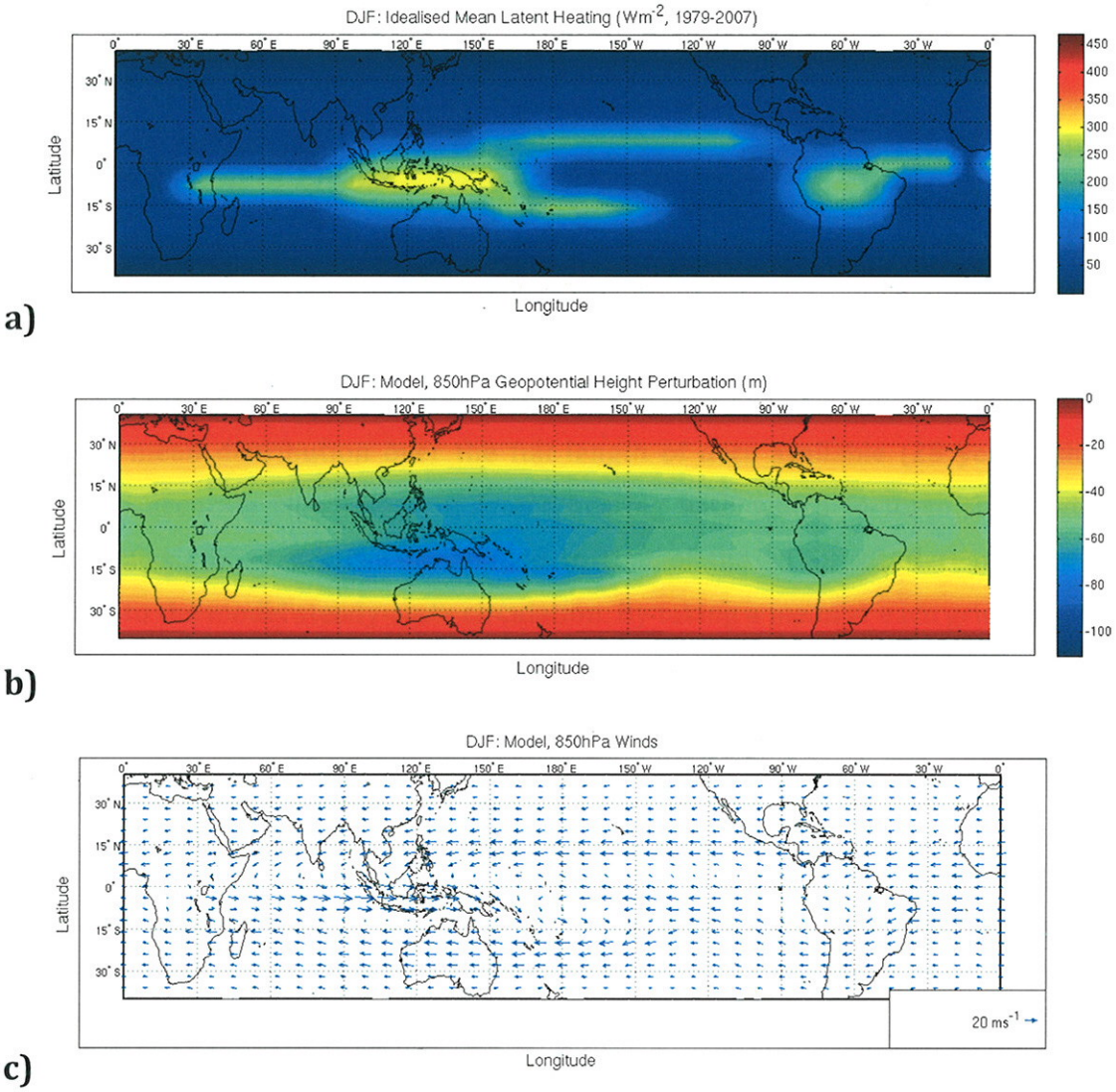

Figure 8: a) Idealised Heating distribution for DJF with the associated b) lower level geopotential height and c) wind.

Both the model response to JJA and DJF heating functions produce encouraging representations of the tropical circulation at low latitudes. However, in subtropical latitudes variations, are small and the model fails to resolve any dominant pressure patterns. The summer hemisphere appears the most poorly resolved as, in both simulations, pressure appears approximately zonally symmetric.

5. Observed Distributions of Latent Heating

In this section the model response to mean CMAP DJF (Figure 9 and 10) and JJA (Figure 10 and 11) precipitation distributions, converted to latent heating are compared to NCEP-NCAR reanalysis fields.

a) Discussion of Errors

With regards to errors, Xie and Arkin (1997) provide a detailed discussion of CMAP errors and measures taken to reduce them. Xie and Arkin (1997) give a 5-10% error in the global average precipitation with less confidence in individual grid points. Efforts to reduce any errors in this study are minimal as a result of the aim and nature of the project. A mean distribution over the full length of data available (28 years) should provide an accurate climatology of latent heating with which to force the model. A similar analysis of errors can be applied to that of the NCEP-NCAR reanalysis data compared to the model steady-state circulation. By taking a mean at each grid point over the same period (1979-2007) we obtain a far more accurate estimate of the global circulation.

b) Magnitude of Model Winds

Comparisons of the magnitude of winds between the model (Figures 9, 10, 11 and 12) and reanalysis (Appendix A: Figures 1 and 2) suggest that the winds produced are not of the same magnitude at either level. Mean and standard deviations of the entire field of wind components, as in Table 2, illustrate this fact.

Both the mean and spread of wind are much larger in the observations at 150hPa and much smaller at 850hPa for both seasons. This is a product of both the two layer approximation and the damping term in the simplified primitive equations, documented in Section 2. Although observations of winds provide evidence to propose a two layer approximation the assumption considers the direction of the winds and not the magnitude.

A constant equal damping, (E=0.03) accounting for friction and cooling, is not physically correct. In the observed flow there is more damping at the lower levels with less in the upper levels. While 850hPa may be above the boundary layer over much of the ocean, the boundary layer is deeper over land due to convective mixing and orographic effects.

Thus large amounts of energy are removed through frictional forces and the winds at the lower levels are weaker. Although mean zonal winds in Table 2 clearly indicate that the model wind magnitude is an intermediate between the 850hPa and 150hPa observed winds the picture is not so clear for the meridional winds. We can account for this in the lower levels by considering the topography of the tropics. Three meridionally orientated regions of high ground intersect the tropics and studies (Slingo et al., 2005, Chakraborty et al., 2002) indicate that these alter the cross equatorial meridional flows of the west Indian Ocean. This appears to account for the strong meridional flow in the model relative to the zonal. Further consideration is given to orography throughout the remainder of this chapter.

Table 2: Means and standard deviations of the magnitude of the wind field in both zonal and meridional wind directions. Values are produced for the model and NCEP winds at 150hPa and 850hPa.

Wind Field (ms^{-1})		**JJA**		**DJF**	
		Mean	**Standard Deviation**	**Mean**	**Standard Deviation**
Zonal	NCEP 850hPa	4.5	3.1	4.3	3.0
	Model	**12.5**	**9.7**	**12.0**	**8.6**
	NCEP 150hPa	16.5	12.0	18.8	13.0
Meridional	**NCEP 850hPa**	**1.5**	**1.4**	**1.2**	**1.1**
	Model	3.4	2.9	3.0	2.7
	NCEP 150hPa	**2.4**	**2.1**	**3.1**	**2.4**

c) Boundary Condition and Subtropical Jet Streams

Some strong vector differences are observed at the north and south boundaries of the model (Figures 9c, 10b, 11c and 12b). These are associated with winds in the subtropical jet stream. However it was not expected that the model would reproduce such winds for a number of reasons. Firstly, the boundary condition of the model sets winds to zero and heating close to the boundary is 'phased out'. Therefore there is little energy provided by the model to force winds at these latitudes. Subtropical jet streams in the observed flow are an effect of the strong temperature gradient between the mid-latitudes and the tropics (Holton, 2006). Thus any jet stream would require a gradient in heating at the boundaries. In experiments with the model it was found that imprinting a uniform cooling over the entire domain to represent radiational cooling induces a gradient in

heating at the north and south boundaries as required. A pressure gradient is produced that induces a subtropical westerly jet. While this may be a familiar feature of the subtropical flow, the pressure gradient producing the flow is induced by the poleward boundary condition rather than an equator-pole temperature gradient. Relative to a model run with no cooling, there appears to be no effect at lower latitudes but to alter the magnitude of winds. An interesting idea would be to impose an observed outgoing longwave radiation field on that of the heating. However this is beyond the scope of the current study and thus any cooling is excluded from further experiments.

d) Orographic effects on low level winds

Vector differences in figure 9c and 11c show significant correlation between land areas and large discrepancies between model simulations and observed winds. This effect appears to be enhanced over much of the tropical mountain ranges. Strong vector differences are observed in association with the Himalayas, the East African Highlands, the Andes, the Indonesian mountains and Australia (Figures 9c, 10b, 11c and 12b). This appears to be a key difference between the 850hPa winds within the model and that of the observed. More details on this topic are discussed in further sections.

e) Simulation Forced by CMAP Mean 1979-2007 DJF Latent Heating

This section provides an analysis of the fields produced by forcing the model with the climatological mean DJF latent heating produced from CMAP in Figure 1b.

The geopotential height field (Figure 9a) shows a more complex picture than that of the geopotential height field produced by the idealised DJF latent heating (Figure 8a), although there are many similarities between the two. Many of the large pressure perturbations are again produced in the summer hemisphere. A broad trough spans the region from Southern India to the central Pacific Ocean; a pattern reproduced in the observed geopotential height field (Appendix A: Figure 1a).

Embedded within the trough is a strong region of low geopotential height produced by a Rossby wave associated with deep convection in the South Pacific Convergence zone (SPCZ). While elongated and constrained to the Southern Hemisphere, there are many similarities between this pattern and the simple symmetric solution produced by Gill (1980). The Rossby wave propagates upstream producing a monsoonal circulation across North Australia and South-Western Indonesia; a characteristic flow in the tropics

during the DJF season. While this appears to be characteristic of the season, strong vector differences in Figure 10c show that the strong low level westerly jet over the Indian Ocean in Figure 10b is in fact weaker in the observations than that produced by the model.

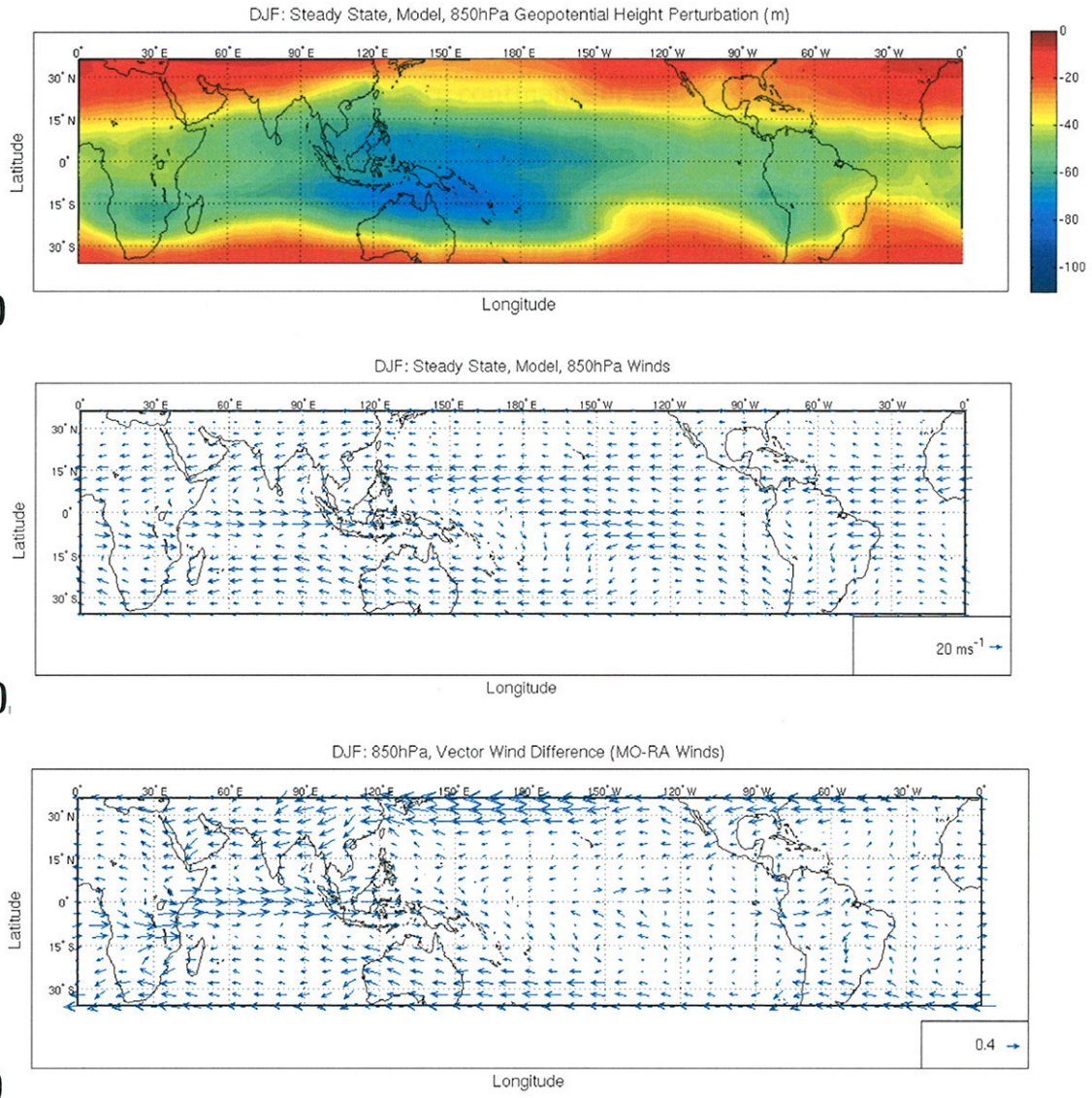

Figure 9: Model simulations forced by latent heating produced from DJF mean CMAP precipitation. Images of 850hPa: Steady-State a) Geopotential height, b) Winds and c) Normalised vector differences (difference = model-reanalysis, 1 indicates large difference between model and reanalysis, 0 indicates no difference).

The westerly jet here extends as far back as western Africa although vector differences again show that this is not in agreement with the observations. Some explanation for this can be found by considering the Indonesian orography. Indonesian mountains

produce large topographically induced frictional forces at low levels. In the observed flow the motion of any equatorial low level jet in these longitudes could be prohibited by the East African Highlands and Indonesian orography. Thus we can attribute to orography, a reduction in the flow relative to that of the Australian monsoon circulation, simulated in the model.

In addition, weaker Rossby waves, defined by low geopotential height in Figure 9a, are centred over the Southern hemisphere continents of Africa and South America. A Rossby wave over South America appears to produce a weak circulation. However this coincides with the Andes, a strong region of orographic friction that will disrupt any wave produced by heating in this region. In fact, Insel et al. (2009) used a regional model to show that the Andes appear to have a strong effect on the regional circulations. They show that a westerly jet is blocked by the presence of topography in the region while also showing that a removal of topography affects precipitation. Strong but relatively incoherent vector differences over the Amazonian basin shown in Figure 9c appear to confirm the orographic blocking of circulation patterns.

Despite a number of significant differences in the low level circulation, mostly associated with orography, there is relatively good agreement between simulated and observed winds over oceans. Subtropical ridges are seen to correlate relatively well with the mean observed field (Appendix A: Figure 1a), despite the boundary conditions. In the Southern Hemisphere ridges in the Indian, East Pacific and South Atlantic Ocean are seen to coincide with the semi-permanent Mascarene High, South Pacific High and St Helena High respectively (Asnani, 2005). In the Northern Hemisphere ridges of high pressure appear to coincide with the Azores High and North Pacific High. Thus, vector differences in Figure 10b indicate regions of strong correlation in these regions.

Although there is an overall general correlate with observed geopotential heights, the model appears to fail to show some of the smaller mean pressure centres such as that over South East Asia and the Middle East in the reanalysis 850hPa geopotential heights (Appendix A: Figure 1a). Some numerical artefacts are produced by the model in East Pacific and South American longitudes. These are associated with the iterative technique of the model and are thus not characteristic of the observed fields.

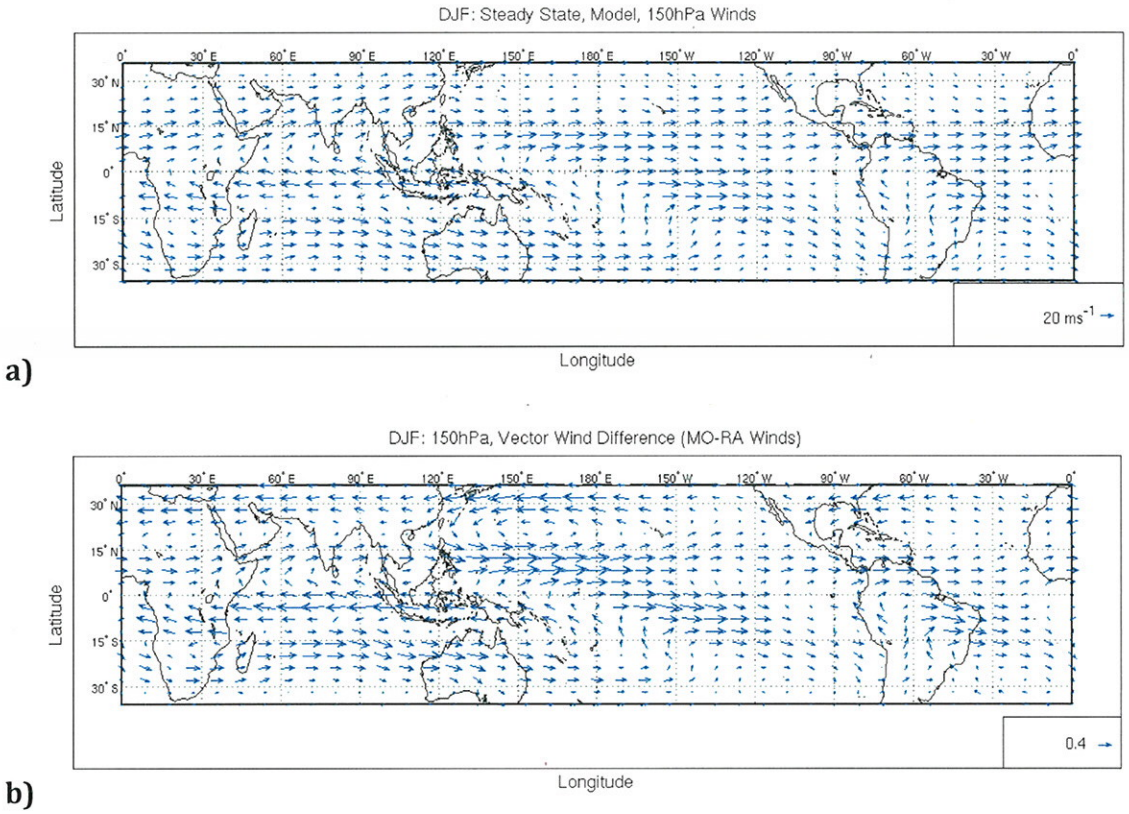

Figure 10: Model simulations forced by latent heating produced from DJF mean CMAP precipitation. Images of 150hPa: a) Steady-State Winds and b) Normalised vector differences (difference = model-reanalysis, 1 indicates large difference between model and reanalysis, 0 indicates no difference).

Vector differences in Figure 10b show that the upper level winds do not correlate well with observations for this season, despite relatively similar pressure patterns. 150hPa geopotential height can be observed as the negative perturbation to that in Figure 9a due to the two layer approximation and an observed climatology can be seen in Appendix A: Figure 1c. At 150hPa a strong upper level high forms in association with the lower level Rossby wave connected with the South Pacific convergence zone. This high appears to induce an overall diverging flow from this region while vector differences in Figure 10c show that this is very different to observations (Appendix A: Figure 1d). Observed winds are in fact relatively calm in this zone as a result of the high geopotential heights pushing much farther north. Here we see another instance where the two layer assumption breaks down. Flow in the eastern Pacific and Atlantic appears to be consistent with the observed flow of Westerlies in this region. Here the influence of subtropical highs and the presence of Westerlies allow subtropical Rossby waves to penetrate equatorial latitudes; a phenomenon described as the equatorial duct.

f) Simulation Forced by CMAP Mean 1979-2007 JJA Latent Heating

Figures 11 and 12 indicate the perturbation in geopotential height, winds and vector differences produced by forcing the model with a JJA heating distribution, as in Figure 1a. Again, as a result of the numerical iterations, the model appears to produce some form of numerical artefact. We see a number of these artefacts created in the geopotential height over much of the Americas and Africa. These are produced by the sharp gradient in the observed forcing in this region. Figure 11a shows a deep low pressure centre associated with latent heating produced in the Indian Monsoon. This is embedded within a deep, broad equatorial trough spanning from West Africa to the Americas.

During the JJA season the most prominent feature in the 850hPa winds is the cross equatorial Somali jet associated with the Monsoonal trough. From Figure 11c we see that the cross equatorial flow in the Somali jet is substantially weaker than that of the reanalysis. Again, orography appears to have a major role in affecting circulation patterns within this area. Chakraborty et al. (2002) showed that removal of the orography in this region substantially alters the jet. With African orography removed there is a reduction in the flow from the south but an increase in the flow from the west. Additionally they show that the removal of orography associated with the Tibetan plateau and the Himalayas substantially decreases the strength of the jet over the Arabian Sea. This is in agreement with the findings of Slingo et al. (2005). In a comparison with the current study it is clear that orography of the East African Highlands play a key role in concentrating the Somali jet. Some strong similarities are observed between Slingo et al. (2005) and the resolution of the Somali jet in the current model simulations. Despite the orographic effects, vector differences (Figure 11c) indicate that the westerly monsoonal inflow jet over India is similar to the reanalysis, although displaced slightly further south. A monsoonal circulation is also observed, similar to the idealised circulation in Section 4, Figure 8c.

Some differences that appear not to be accounted for by orography are that of a weak westerly jet in the West Pacific and to a lesser extent, westerly winds off the East equatorial coast of South America. This appears to be associated with strong regions of the ITCZ. This in agreement with Clarke (1994) who showed that weak westerly propagating Rossby waves induced a westerly jet. However, little explanation can be

offered from either the current study or that of Clarke (1994) for the significant difference from observations.

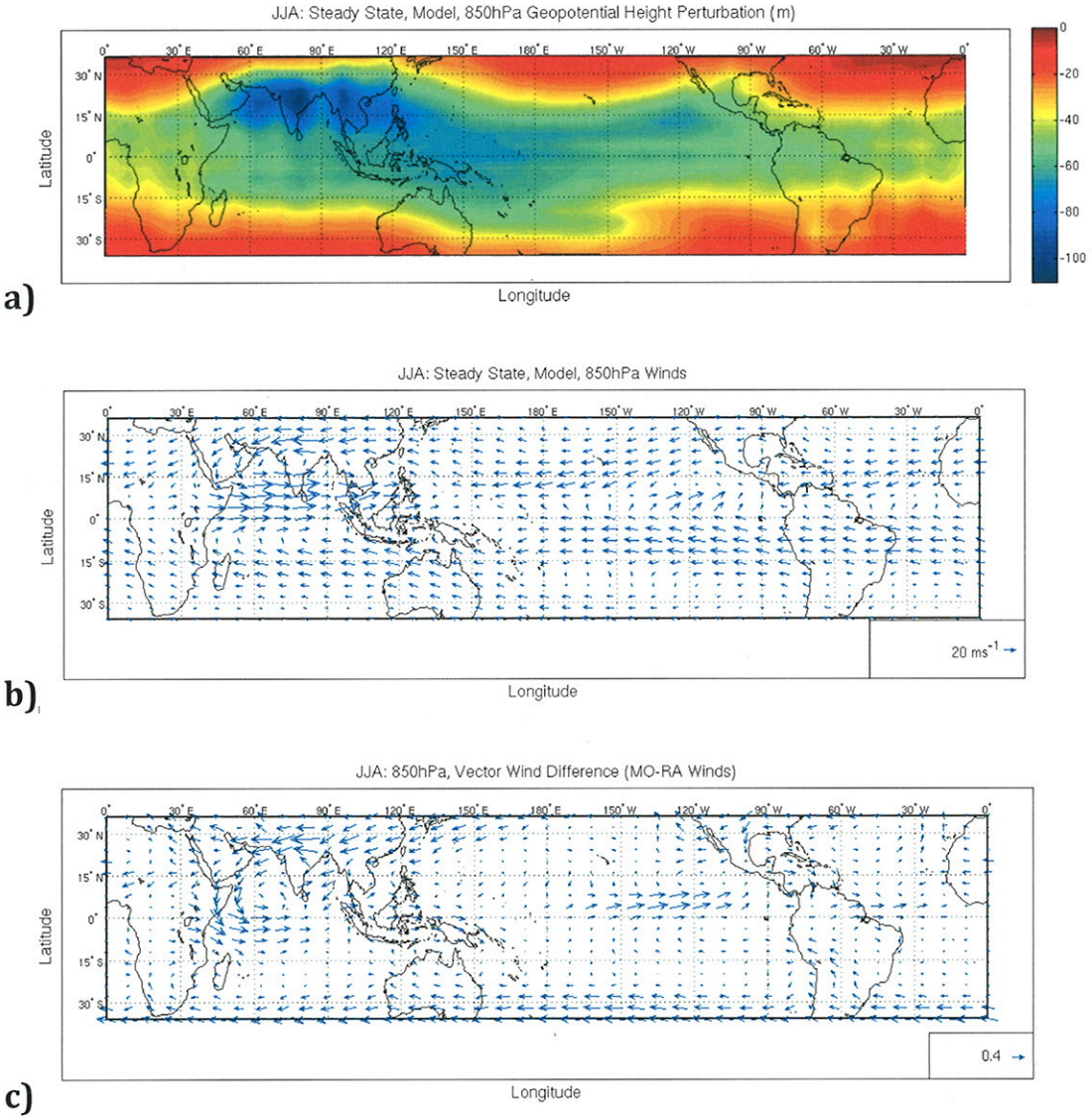

Figure 11: Model simulations forced by latent heating produced from JJA mean CMAP precipitation. Images of 850hPa: a) Steady-State Geopotential height, b) Winds and c) Normalised vector differences (difference = model-reanalysis, 1 indicates large difference between model and reanalysis, 0 indicates no difference).

Overall, vector differences in Figure 11c show a relatively strong correlation between the low level winds and observations. Strong subtropical ridges coincide with areas associated with the Azores high and the North Pacific High in the northern hemisphere and the Mascarene high, South Pacific high and St Helena high in the Southern Hemisphere. Over much of the Pacific Ocean and Atlantic we find easterlies in agreement

with the observed wind fields that appear to track the circulation in these high pressure regions.

It appears that there is strong convergence produced at low levels over much of the tropics. Figure 12a, indicates a divergent motion aloft produced by the model. This coupling of convergence and divergence can be likened to the rising branch of the Hadley Cell.

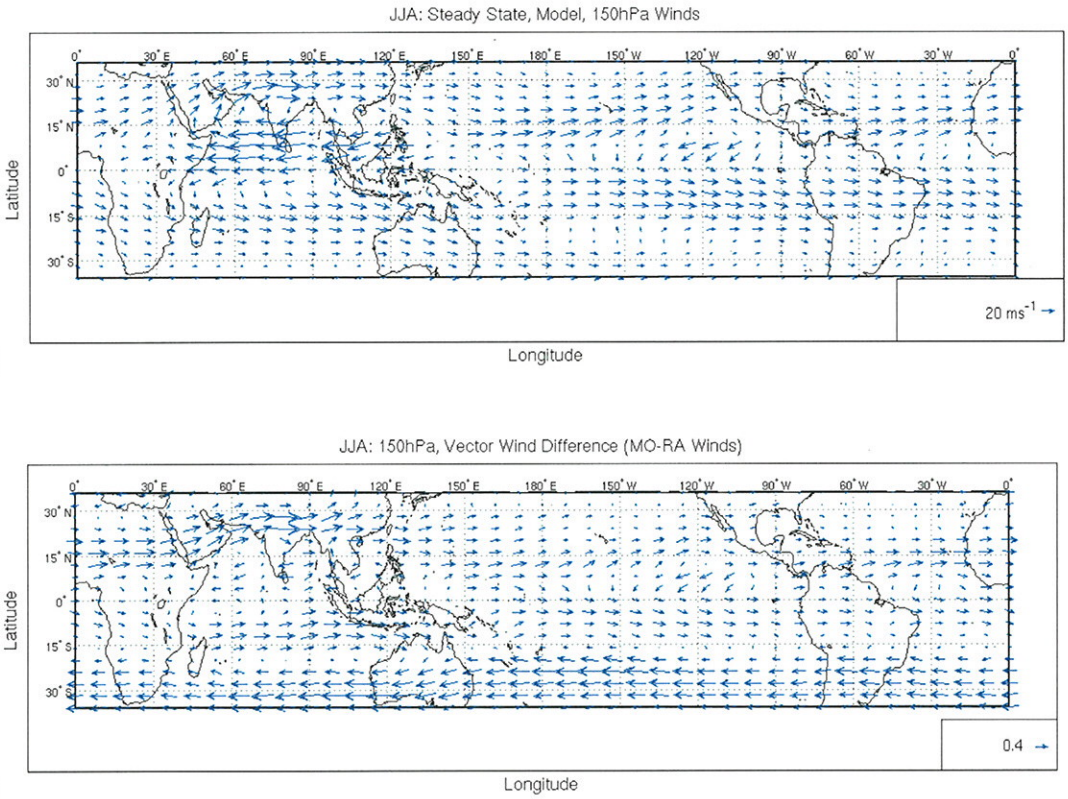

Figure 12: Model simulations forced by latent heating produced from JJA mean CMAP precipitation. Images of 150hPa: a) Steady-State Winds and b) Normalised vector differences(difference = model-reanalysis, 1 indicates large difference between model and reanalysis, 0 indicates no difference)..

As with DJF, the two level model allows us to view the negative of the pressure patterns in Figure 11a as the 150hPa geopotential heights. A strong region of high pressure in the upper levels appears to coincide with the Tibetan high. This is associated with a strong westerly jet that is in agreement with the observations, as shown by the vector differences in Figure 12b. This jet is a reproduction of the most prominent feature of the tropical upper level flow in the JJA season, the Tropical Easterly Jet. Geopotential height patterns confirm that upper level convergence associated with the jet exit appears to

suppress the African monsoon system as shown by Webster and Fasullo (2003). Thus it does not appear that a monsoon circulation is produced in the model over this region.

While the African easterly jet appears to be resolved relatively well by this model, Figure 11b vector differences show that much of the rest of the flow is in poor agreement with the observations. Much of this is due to a displacement of the subtropical westerly jet towards the equator. Specifically in the Northern Hemisphere this jet is observed as a result of the land sea contrast. Thus, the lack of land surfaces in the model has some effect on this shift. This is also due in part to the boundary condition which forces flow at the boundaries to zero.

6. Conclusions

The aim of this study was to build and develop a simple numerical model analogous to the analytical model produced in Gill (1980). Simulations forced by various distributions of heating were analysed to assess the capability of this model in reproducing the tropical general circulation.

A simulation forced with a simple symmetric distribution of latent heating reproduces the classic Kelvin-Rossby wave couplet produced in Gill (1980). Some numerical artefacts are observed, although they have little effect on the model output. Thus it is verified that the numerical model reproduces Gill's (1980) analytical solutions. When forcing the model with a combined heating function, analogous to the JJA distribution of latent heating, circulations patterns agree with the second of Gill's (1980) solutions, documented in Section 1. However, by displacing the symmetric heating function North, it appears more applicable to the general circulation during the JJA season than Gill's. It is shown that this very simple idealisation produces many features of the JJA season general circulation. In light of these observations it was concluded that the model could have the capability to reproduce more of the tropical general circulation with improved forcing fields.

Therefore, idealised distributions of the JJA and DJF seasons latent heating were produced by combining line and symmetric functions. Model simulations, using JJA heating, improved on the combined (Symmetric and Line) heating simulation by providing more structure to the flow. Some subtropical ridges appear to be evident in

this idealised version and the equatorial trough broadened. However, westerly flow associated with the monsoon appears to create a strong meridional flow from the north, a feature not produced in the observed winds. Both JJA and DJF simulations produced little variation in pressure in the Winter Hemisphere; a pattern not seen in the reanalysis fields. This occurred as a result of minimal heating in the Winter Hemisphere. Much of the flow forced by idealised heating distributions showed similarity to observed seasonal general circulations. Monsoonal circulations and pressure systems appeared to be produced relatively accurately considering the idealised nature of the simulations.

An observed climatology, using CMAP precipitation as a proxy for latent heating, produced simulations with much similarity to the observed fields. Some of the assumptions made for this simple model are not particularly accurate; in particular the two layer assumption. Although theoretically appropriate when considering conceptual flows in the tropics such as the Walker Cell and Hadley Cell, the assumption does not allow for an observed variation in magnitude between upper and lower levels. As a result, it is seen that the magnitude of the winds is inaccurate in model simulations. This is also a result of an equal damping term in the shallow water equations between both layers. This term does not account for the variation in frictional and radiative forcing between the layers. It is proposed that the two level approximation be discarded in favour of a multi-level model in further work. There is also the possibility with such a model that other tropical general circulation features would be resolved. For example, no model simulation in this study predicted the existence of the African easterly jet.

Discounting magnitude, much of the lower level flow appears to be in agreement, despite some discrepancies attributed, in most cases, to orography. Model simulations indicate a number of low level westerly jets produced in association with an inflow into regions of high heating. These are similar to that produced by a simple symmetric distribution of heating in Gill (1980). However, these are in most cases not observed or have a much weaker magnitude in the reanalysis winds. In a number of cases this error can be accounted for by considering the topography over which the low level jet flows. This is not true in all cases. Reasons for these discrepancies appear to be beyond current understanding. One of the most prominent features of the low level winds, the cross equatorial Somali jet, appears to be weaker due to orography. However, it is compared to a study by Slingo et al. (2005) where orography is omitted. Many similarities are

found between this study and Slingo et al. (2005). While southerly inflow to the Monsoon is weaker there is still a similar inflow. It is proposed that an observed field of orography could be included to the forcing. Orography forces vertical motion at the lower levels and thus would force the flow in a similar way.

The model produces numerical artefacts when forced by sharp gradients of heating. A simple improvement to this would be to alter the resolution of the model so that sharp gradients in the heating are smoothed out.

Observed discontinuities in the subtropics are a result of the boundary condition to the North and South. A complex improvement to the boundary condition could involve removing boundaries and coupling this model to a mid-latitude general circulation model. However, this option would not preserve the simplicity of the model and thus simpler boundary conditions should be explored first. Imposing a simple temperature gradient at the boundaries would replicate the difference in temperature between the tropics and mid-latitudes. This would likely produce a westerly subtropical jet that in turn, would resolve subtropical high pressure systems more accurately. Imposing a constant longwave cooling was also examined and the implications were that it created a subtropical jet. However this is in fact a result of the current boundary condition. Combining the temperature gradient with the application of an observed long wave cooling would likely improve both circulation in the subtropics and tropics.

It may be conducive to examine the flow produced by mean equinoctial heating. However as this is the transition phase in the tropics, it is likely there is a much larger interannual variability in precipitation and thus latent heating. Therefore flow produced by the model would have strong variations from the reanalysis winds.

Whilst the model has a number of flaws, with the proposed improvements it is thought that much of the tropical general circulation should be resolved in the model. Thus, it is concluded that the model could be used as a simple, reliable framework for studying the response of the atmosphere to heating in the tropics.

Acknowledgements

I thank my advisor, Dr Pete Inness for his guidance over the duration of the project. In particular I thank him for insightful discussions and assistance with programming in FORTRAN.

References

Asnani, G. C., 2005: *Tropical Meteorology: Volume 1.* 2nd Edition. Praveen Printing Press, 1202pp.

Bjerknes, J., 1969: Atmospheric Teleconnections from the Equatorial Pacific. *Mon. Weather Rev.,* **97 no. 3,** 163-172.

Butler, A. H., Thompson, D. W. J. and Heikes, R., 2010: The Steady-State Atmospheric Circulation Response to Climate Change-like Thermal Forcings in a Simple General Circulation Model. *J. Climate,* **23**, 3474–3496.

Chakraborty, A., Nanjundiah, R. S. and Srinivasan, J., 2002: Role of Asian and African Orography in Indian Summer Monsoon. *Geophys. Res. Lett.,* **29**, 1-4.

Clarke, A., 1994: Why Are Surface Equatorial ENSO Winds Anomalously Westerly Under Anomalous Large Scale Convection?. *J. Climate,* **7**, 1623–1627.

Gill, A. E., 1980: Some simple solutions for heat-induced tropical circulation. *Q. J. Roy. Meteor. Soc.,* **106,** 447-462.

Hadley, G., 1735: Concerning the cause of the general trade winds. *Phil. Trans.,* **39**, 58-62.

Halley, E., 1686: An Historical Account of the Trade Winds, and Monsoons, observable in the Sea between and near the Tropicks with an attempt to assign the Physical cause of the same Winds, *Phil. Trans.,* **16,** 153-168.

Hastenrath, S., 1996: *Climate dynamics of the Tropics.* Kluwer Academic Publishers, 488pp.

Holton, J. R., 2004: *An Introduction to Dynamic Meteorology.* Fourth Edition. Elsevier Academic Press, 535pp.

Houze, R. A., Chen. S. S., Kingsmill. D. E., Serra. Y. and Yuter. S. E., 2000: Convection over the Pacific Warm Pool in relation to the Atmospheric Kelvin-Rossby Wave*, *J. Atmos. Sci.,* **57**, 3058-3089.

Insel, N., Poulsen, C. J. and Ehlers. T. A., 2009: Influence of the Andes Mountains on South American moisture transport, convection, and precipitation. *Clim. Dyn.,* **35**, 1477-1492.

Kalnay, E., et al., 1996: NCEP-NCAR 40 Year Reanalysis Project. *Bull. Amer. Meteor. Soc.*, **77**, 437-471.

Katayama, A., 1964: On the Heat Budget of the Troposphere Over the Northern Hemisphere, Ph. D. thesis, Tohoku University, Japan, 264pp.

Krishnamurti, T. N. and Bhalme, B. N., 1976: Oscillations of a Monsoon System. Part 1. Observational Aspects. *J. Atmos. Sci.*, **33**, 1937-1954.

Lee, S.-K., Wang, C. and Mapes, B. E., 2008: A Simple Atmospheric Model of the Local and Teleconnection Responses to Tropical Heating Anomalies. *J. Climate*, **22**, 272-284.

Marshall, J. and Plumb, R. A., 2007: *Atmosphere, Ocean and Climate Dynamics, An Introductory Text.* Elsevier Academic Press, 344pp.

Phillips, N. A., 1963: Geostrophic motion. *Rev. Geophys.*, **1**, 123–176.

Roundy, P. E. and Lynn M. G.-V., 2010: Variations in the Flow of the Global Atmosphere Associated with a Composite Convectively Coupled Oceanic Kelvin Wave. *J. Climate*, **23**, 4192–4201.

Slingo, J., Spencer, H., Hoskins, B., Berrisford, P. and Black, E., 2005: The meteorology of the Western Indian Ocean, and the influence of the East African Highlands. *Phil. Trans.*, **363**, 25-42.

Webster, P. J. and Fasullo. J., 2003: Monsoon: Dynamical Theory. *Volume Three*, Holton. J. R., Curry, J. A. and Pyle, J. A., Vol. 3, *Encyclopedia of Atmospheric Sciences*. Elsevier Academic Press, 1370-1386.

Webster. P. J., 1972: Response of the Tropical Atmosphere to Local, Steady Forcing. *Mon. Weather Rev.*, **100,** 518-541.

Wu, Z., Sarachik. E .S. and Battisti. D. S., 2000: Thermally Driven Tropical Circulations Under Rayliegh Friction and Newtonian Cooling. *J. Atmos. Sci.*, **58**, 724-740.

Xie P., and Arkin, P. A., 1997: Global precipitation: a 17-year monthly analysis based on gauge observations, satellite estimates, and numerical model outputs. *Bull. Amer. Meteor. Soc.*, **78**, 2539-2558.

Appendix A

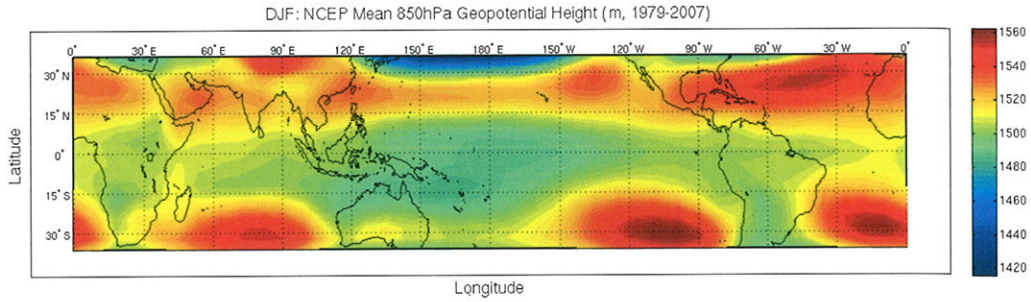

a)

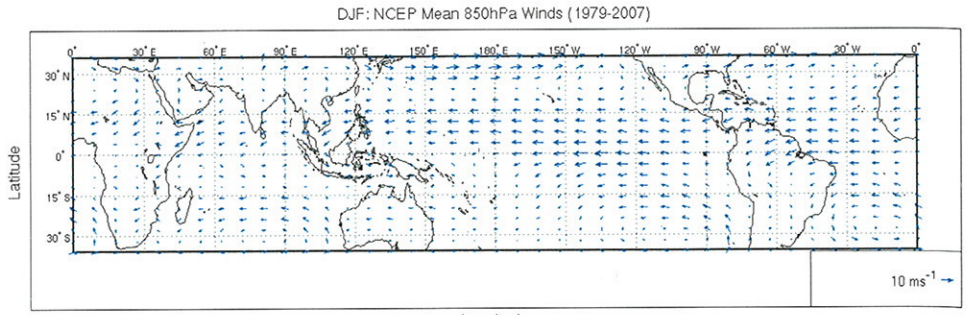

b)

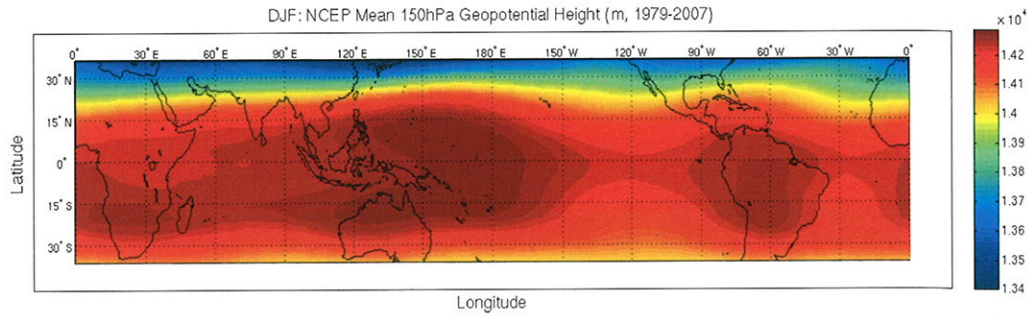

c)

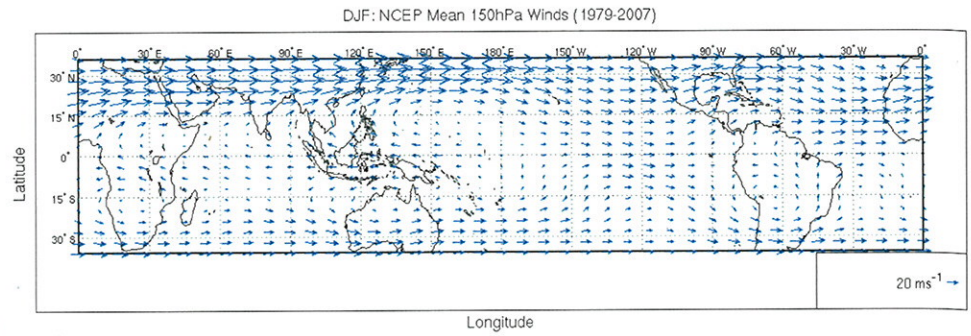

d)

Appendix A, Figure 1: NCEP-NCAR reanalysis DJF season a) 850hPa Geopotential Heights, b) 850hPa winds, c) 150hPa Geopotential Heights, d) 150hPa winds.

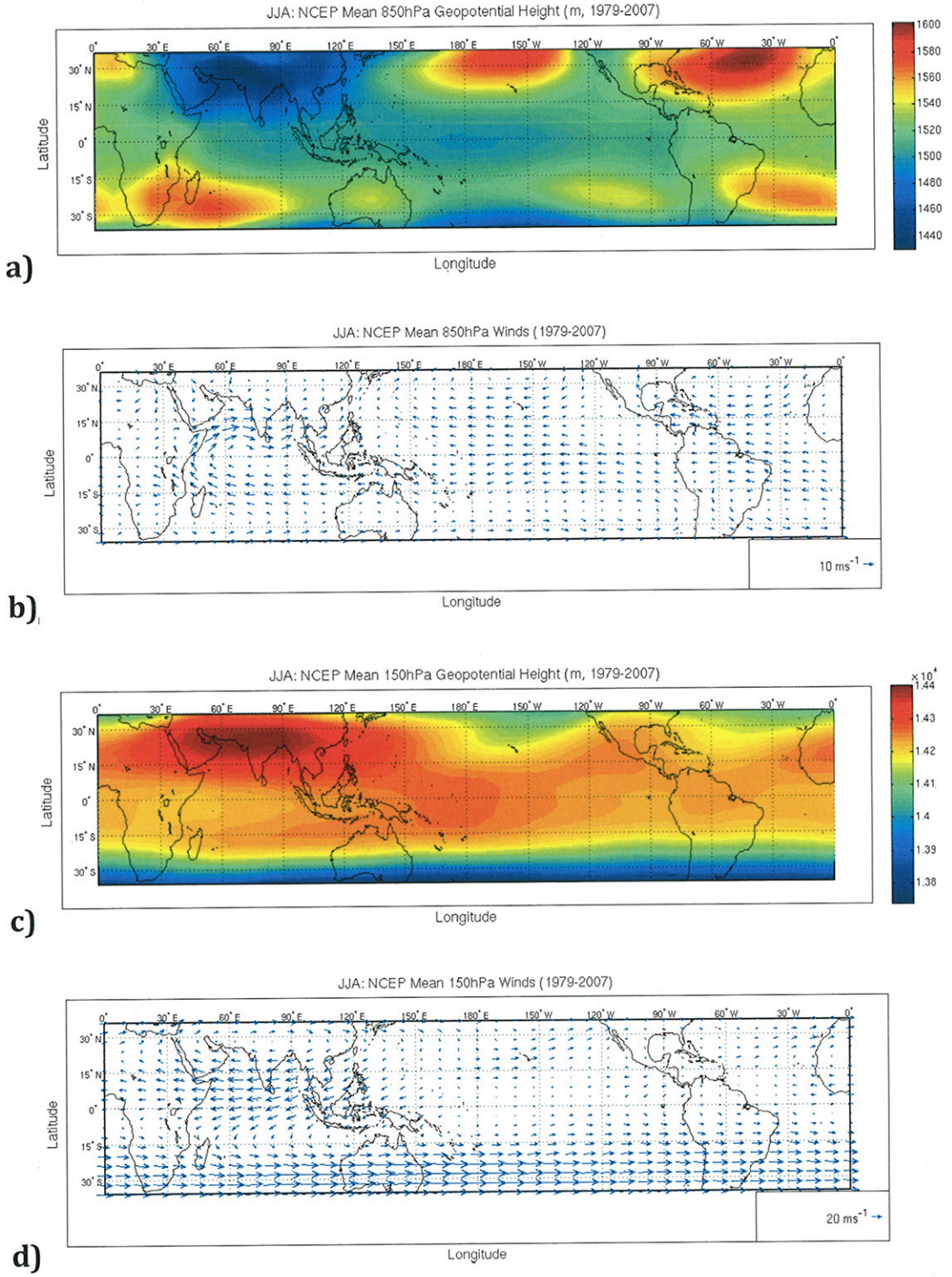

Appendix A, Figure 2: NCEP-NCAR reanalysis JJA season a) 850hPa Geopotential Heights, b) 850hPa winds, c) 150hPa Geopotential Heights, d) 150hPa winds.